International Journal of Control and Automation
Vol.10, No.8 (2017), pp.1-12
http://dx.doi.org/10.14257/ijca.2017.10.8.01

Finite Element Simulation and Experimental Study on Vibration Effect of Defect Position for Cylindrical Roller Bearing

Xia Yang[1], Chuang Yan[1, 2] and Yachao Li[1]

[1]*Shanxi Provincial Key Laboratory of Metallurgical Device Design Theory and Technology, Taiyuan University of Science and Technology, Taiyuan Shanxi, 030024, PR China*
[2]*BAIC Yinxiang Automotive Co., Ltd., Chongqing, 401520, PR China*
**Corresponding author's email: yanchuang33@163.com*

Abstract

Aiming to local defect fault of inner and outer race of roller bearings ,the numerical models of rolling bearings with different local defect fault poisons are established, through the simulation with software of ABAQUS, the contact stress and vibration characteristic curves of rolling bearings are obtained. The vibration test experiments for different defect positions on the inner race are carried out with the bearing vibration measuring instrument, which verifies the correctness and effectiveness of the analysis models. The theoretical analysis and experimental results show that the vibrations also exists in the bearings without defect, and the existence of local defects make bearing stress fluctuation increase, thereby deepening the vibration of the bearing. When local defect is located in the middle of the bearing inner or outer race, the stress fluctuation and the vibration impulse of the bearing are the largest, and also the vibration amplitude.

Keywords: *roller bearing; defect position; vibration simulation; vibration test experiment*

1. Introduction

Roller bearings are the key component of rotating machinery. The defects of roller bearing will seriously affect the vibration of the bearing, thus affect the normal operation of the bearing [1]. The outer race of bearing is the most defective part; defects in different position have different vibration effect on bearing. The study on the vibration characteristics of defective bearing is beneficial to the bearing life. Therefore, the analysis on vibration characteristics to the bearing with different defect positions is necessary.

Recently, scholars from home and abroad did a lot of research on the dynamical characteristics of rolling bearings with local defect. Mcfadden and Smith researched on the vibration response of roller bearings single-point or multi-point defect [2]. Zhang Lele simulated the stress influence of bearing with pitting defect using the software of ANSYS [3]. Mikola and Sopanen simulated the stress distribution of bearing with defect using the software of ADAMS [4]. Zhu Zhifang took a dynamical simulation to the bearing with defect in the middle of outer race, and obtained the vibration influence characteristic of speed and radial load [5]. Zhang Genyuan took a multi-body dynamical simulation to the bearing with point defect in the middle of race [6]. Yang Yang took a dynamical analysis to the bearing with point erosion defect in the outer or inner race, and carried out the stress and vibration characteristic [7]. Dong Yabin simulated and analyzed the vibration frequency component of single local defect on rollers [8]. Zhu Chengjiu simulated and obtained the stress distribution and vibration characteristics when defect occurred on the races or rollers [9]. Zhang Hongxing built the defect simulation and diagnosis system based on software of LABVIEW, which consisted of defect simulation test bench, vibration signal detection circuit and defect diagnosis process [10]. Wang Xing proposed a

ISSN: 2005-4297 IJCA

method of rolling bearing fault diagnosis based on time-frequency feature parameters [11]. Inconclusion, these studies mostly researched on bearing with single-point or multi-point defect; however, there was no research on bearing with different local defect poisons.

The cylindrical roller bearing NU308E is used as simulation model. The numerical models of bearing with different local defect fault poisons are established, through the simulation with software of ABAQUS, the contact stress and vibration characteristic curves of rolling bearings are obtained.

2. Defect Frequency

When defect occurs on the inner race, the defect frequency is [12]:

$$f_0^i = \frac{Z}{2} \cdot \left(1 + \frac{D_w}{D_j} \cdot \cos\alpha\right) \cdot f_r \tag{1}$$

When defect occurs on the outer race, the defect frequency is:

$$f_0^o = \frac{Z}{2} \cdot \left(1 - \frac{D_w}{D_j} \cdot \cos\alpha\right) \cdot f_r \tag{2}$$

where Z is the number of rollers; D_w is the diameter of roller; D_j is the pitch diameter of bearing; α is the contact angle between roller and race; f_r is the revolving velocity of bearing.

3. Establish Finite Element Model

The geometrical parameters of bearing NU308E are shown in Table 1 [13].

Table 1. The Main Parameters of Bearing NU308E

Project	Parameter
Inner diameter of bearing (*d*)/*mm*	40
Width of bearing(*B*)/*mm*	23
Outer diameter of bearing (*D*)/*mm*	90
Diameter of outer race (D_o)/*mm*	74
Diameter of inner race (d_i)/*mm*	52
Length of roller (*L*)/*mm*	12.4
Diameter of roller (D_w)/*mm*	13
Number of rollers (*Z*)	12
Poisson's ratio of bearing material (*v*)	0.3
Elastic modulus of material (*E*)/MPa	$2.07e^5$

According to the bearing parameters, three dimensional models of cylindrical roller bearing with and without local defectis established using the software of Soldworks, as shown in Figure 1. The positions of middle defect, defect 1 and defect 2 on the outer race are shown in Figure 1 (a), and the dimensions of all the defects are $2mm \times 2mm \times 1mm$ (Length × Width × Depth), the node C, D, and E are taken as the reference points of analysis [14]. Figure 1 (b) and (c) show the positions of middle and edge defects on inner race, whose dimensions are the same as the defects on the outer race. Figure 1 (d) shows the mesh model of the bearing, Y indicates radial direction, and Z indicates axial direction.

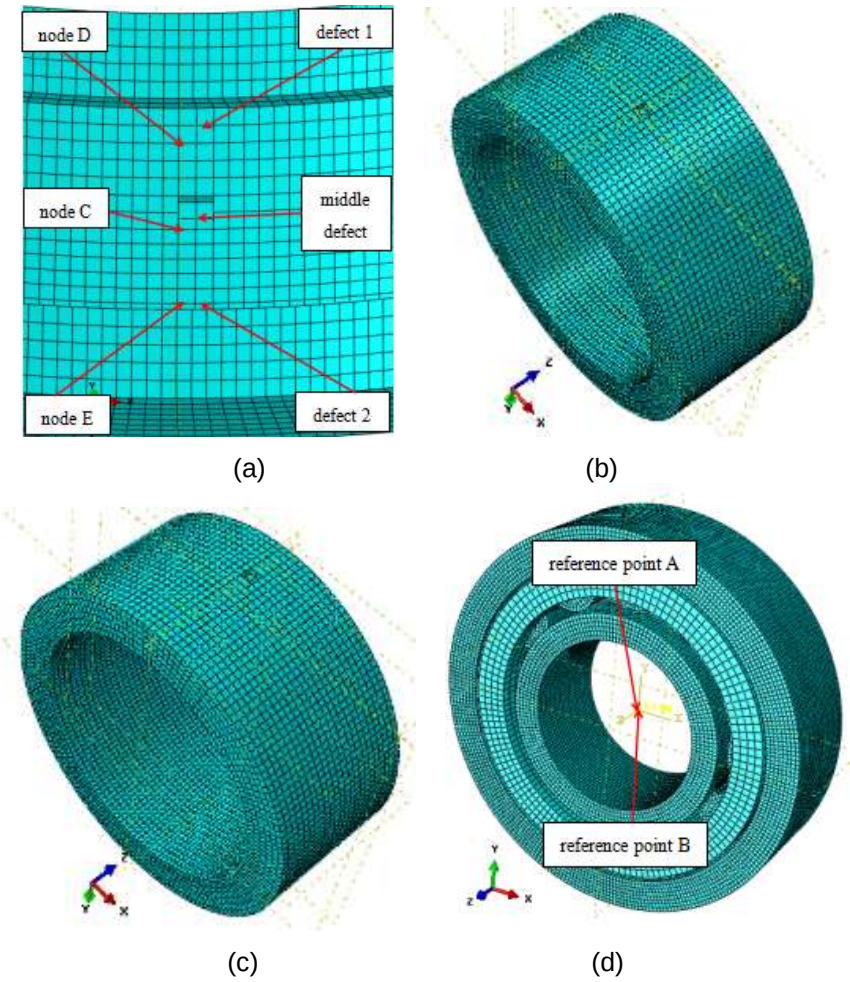

Figure 1. Discrete Models: (a) Defective Outer Race, (b) Middle Defect on Inner Race, (c) Edge Defect on Inner Race, (d) Mesh Model of Bearing

Table 2 shows the reference points. Node C, D, and E are taken as reference points of stress analysis and point A (the rigid reference point of inner surface of inner race) as reference points of speed analysis when defects occur on the outer race. Point B (the rigid reference point of outer surface of outer race) is taken as reference point of speed analysis, when defects occur on the inner race.

Table 2. Reference Point of Analysis

Outer Race			Inner Race	
Defect position	Reference point of stress analysis	Reference point of speed analysis	Defect position	Reference point of speed analysis
Defect 1	Node C	Point A	Normal	Point B
Middle defect	Node D	Point A	Middle defect	Point B
Defect 2	Node E	Point A	Edge defect	Point B

4. The Result of Simulation

4.1. Outer Race with Defects

The boundary conditions and interaction are as follows: inner surface of inner race and outer surface of outer race are taken as rigid bodies; point A and B are taken as rigid reference point of inner and outer race, respectively. Full constraints are applied on the

outer surface of outer race. The freedoms of axial rotation and radial movement of point A are reserved only. There is no constraint on the cage. The general contact manner is used, the tangential friction coefficient between roller and inner and outer race is 0.1, and between roller and cage is 0.05. Hard contact was applied to the normal direction contact. The radial force and revolving speed are 15000 N and 2400 r/min, which are applied on point A [15, 16].

4.1.1. Contact Stress Analysis

Figure 2 shows the contact stresses of reference nodes. From Figure 2 (a), we know that, the stress fluctuation also exists in the bearing without defect; and the existence of local defects make bearing stress fluctuation increase, meanwhile, a new stress fluctuation appears at the time of no stress fluctuation. It can be seen that the variation law of stress of node is changed by the defect on the outer race, which makes the vibration and shock suffered by bearing increase. The increase of vibration and shock will lead to the extending of defect area, thereby the bearing vibration increase ulteriorly. Figure 2 (b) shows the contact stresses of node C, D and E, which represent the positions of middle defect, defect 1 and defect 2, respectively. The maximum contact stresses of the three situations are 1100 MPa, 1550 MPa and 1150 MPa. It can be resulted that the stress fluctuation of node D is the largest, which means that the vibration and shock suffered by outer race is the largest when defect occurs on the middle of outer race. As the position of defect moves to the edge of outer race, the fluctuation amplitude of stress decreases.

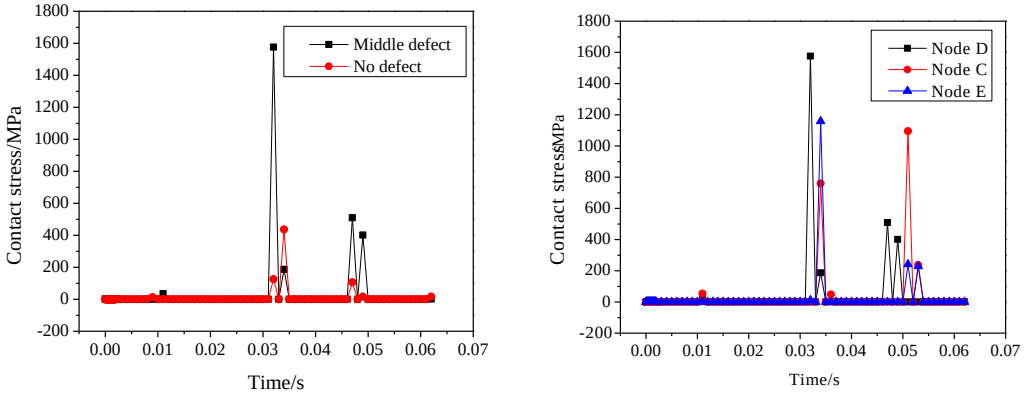

(a) (b)

Figure 2. Contact Stress: (a) Node D, (b) Reference Nodes

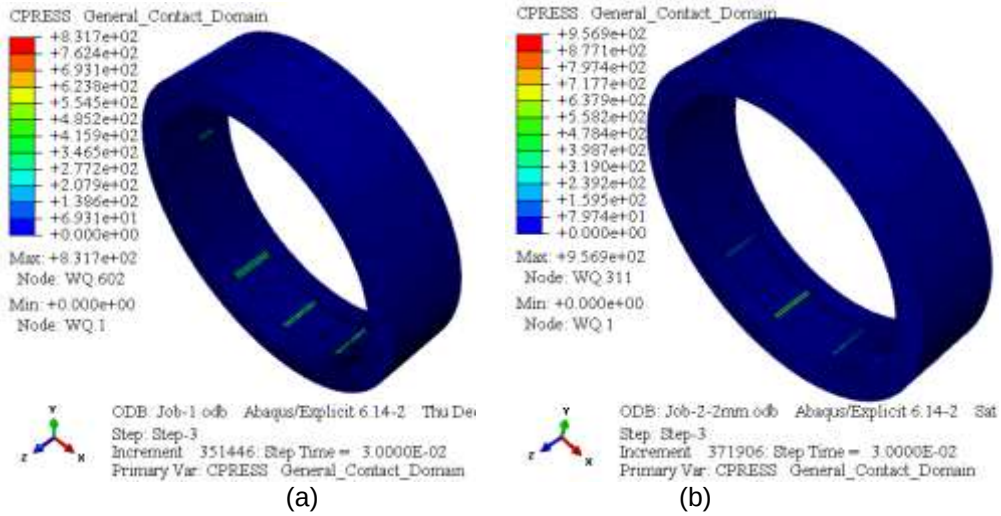

(a) (b)

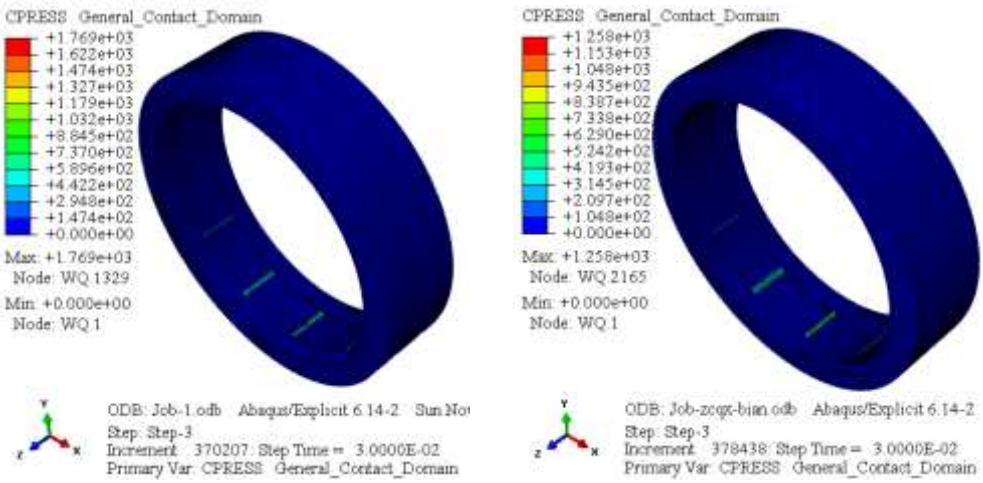

(c) (d)

Figure 3. Contact Stress of Outer Race at 0.03s: (a) No Defect, (b) Defect 1, (c) Middle Defect, (d) Defect 2

Figure 3 shows the cloud picture of contact stress at any time (0.03s) when there are different position's defects on the outer race. From Figure 3, we know that, the half bottom of the outer race is the loaded area, the contact region between outer race and roller is rectangular. When outer race has no defect, defect 1, middle defect and defect 2, the maximum contact stress are 831Mpa, 1258 Mpa, 1769 Mpa and 956 Mpa. It can be resulted that the maximum contact stress of outer race increases significantly when the defect occurs on the outer race. The increased amplitude of contact stress is the largest when the position of defect is in the middle, and the increased amplitude decreases along the axial direction. This result is consistent with the analysis in Figure 2.

4.1.2. Vibration Analysis

Table 3 shows maximum radial displacements of reference nodes. From Table 3, we know that node closer to the defect has the larger radial displacement in any defect situation. To the same node, the node closer to the defect position has the larger radial displacement.

Table 3. The Maximum Radial Displacement of Reference Nodes

Reference node / Defect situation	Node C	Node D	Node E
Defect 1 / mm	0.0069	0.00686	0.00616
Middle defect / mm	0.0052	0.01	0.0054
Defect 2 / mm	0.007	0.0077	0.0089

Figure 4 shows the displacement curve of reference nodes. It can be seen from Figure 4 and Table 3, when the defect positions coincide with the reference nodes, the reference nodes C, D and E have the largest radial displacement, 0.0069 mm, 0.01mm and 0.0089 mm, respectively. The node D has the largest radial displacement; it means that the shock and vibration suffered by outer race is the biggest when defect occurs in the middle of outer race, and smaller when defect occurs on the edge of outer race. The mainly reason is rollers of the middle part bear the most force during working, that make the stress fluctuation and displacement increase, when defect occurs in the middle of outer race.

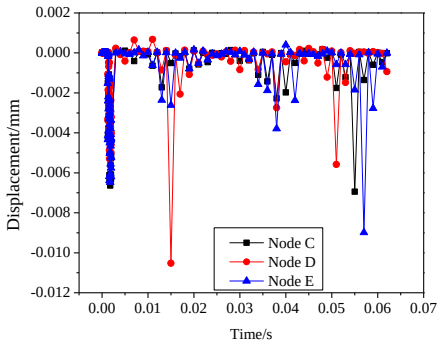

Figure 4. The Displacement Curve of Reference Nodes

The data of Y-direction acceleration of point A (rigid reference point of inner race) is taken to do fast Fourier transform (FFT). The sampling frequency is 1000 Hz, and the number of sampling points is 60. The data in Table 1 and the revolving speed are taken into equation (2), from which the defect frequency of the outer race can be obtained, and the value is 190.56 Hz. Figure 5 shows the FFT of Y direction acceleration of point A at normal situation, defect 1 situation, middle defect situation and defect 2 situation.

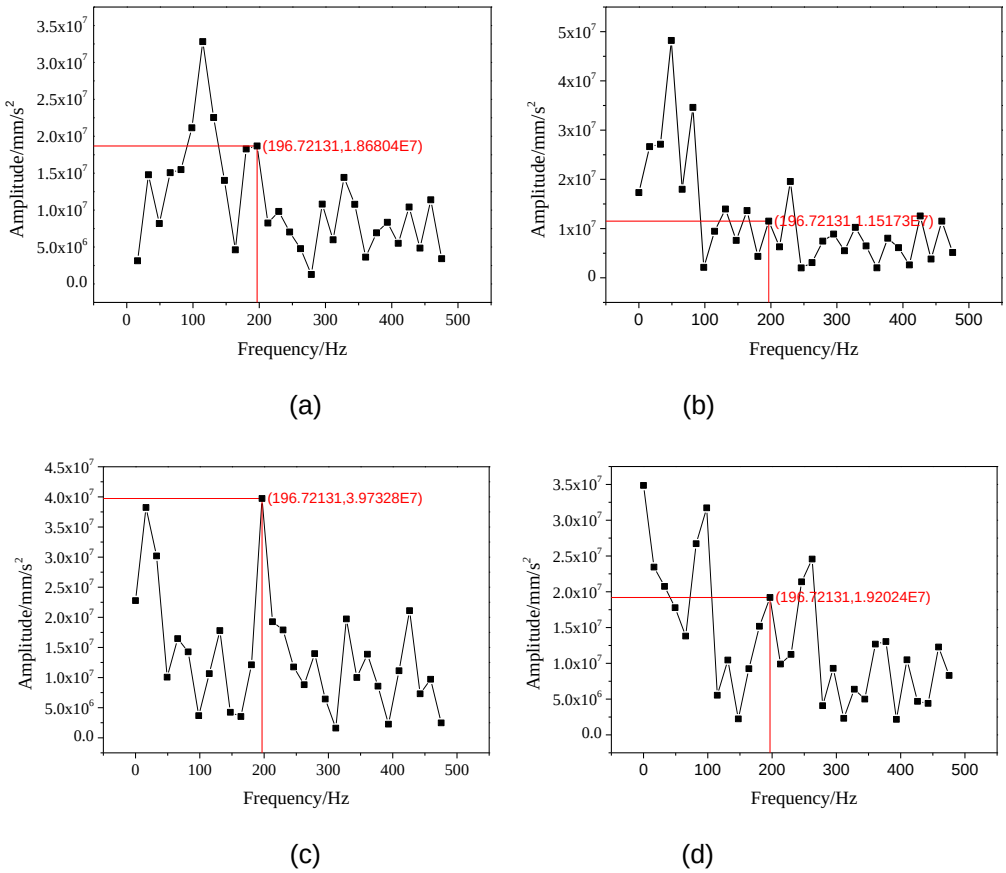

Figure 5. FFT of Y Direction Acceleration of Point A: (a) Normal Situation, (b) Defect 1 Situation, (c) Middle Defect Situation, (d) Defect 2 Situation

It can be seen from Figure 5, the amplitudes at 196.7 Hz are different when FFT is applied to acceleration of point A. The amplitudes at 196.7 Hz of normal situation, defect 1 situation, middle defect situation and defect 2 situation are 1.1×10^7 mm/s^2, 1.86×10^7

mm/s^2, 3.97×10^7 mm/s^2 and 1.92×10^7 mm/s^2. The amplitudes increase at defect frequency, and the increased value when defect occurs on the edge of outer race is smaller than the one when defect occurs in the middle of outer race. The error between defect frequency (196.7 Hz) and theoretical frequency (190.56Hz) is 3%, which indicates that the FFT of Y direction acceleration of point A is effective. But, there are other frequency components, whose amplitude is larger.

4.2. Inner Race with Defects

Due to the limitation of the load range of experimental apparatus, and in order to ensure the effectiveness of comparison between simulation results and experimental results, the same conditions as experiment are adopted to the simulation of defective inner race. When simulate the defective inner race, rotation around axis for inner race and radial displacement for the outer race are reserved only. The force of 250 N is applied to the outer race, the revolving speed of 1800 r/min is applied to the inner race, and the other conditions and material properties are consistent with the defective simulation of outer race.

4.2.1. Contact Stress Analysis

Figure 6 shows the cloud picture of contact stress of inner race of normal situation, edge defect situation and middle defect situation at the time of 0.013s. It can be seen from Figure 6, the maximum contact stresses of the three situations are 110 MPa, 184 MPa and 255 MPa, respectively. It can be resulted that defect on the inner race make the contact stress of inner race increase, and the middle defect on the inner race make amplitude larger.

4.2.2. Vibration Analysis

The data in Table 1 and the revolving speed are taken into equation (1), from which the defect frequency of the inner race can be obtained, and the value is 217.1 Hz. The sampling frequency is 1000 Hz, and the number of sampling points is 60. Figure 7 shows the FFT of Y direction acceleration of point B at normal situation, edge defect situation and middle defect situation.

It can be seen from Figure 7, the amplitudes at 213Hz are different when FFT is applied to velocity of point B. The amplitudes at 213 Hz of normal situation, edge defect situation and middle defect situation are 6.6 mm/s, 31 mm/s and 52 mm/s. The amplitudes increase at defect frequency, and the increased value when defect occurs on the edge of inner race is smaller than the one when defect occurs in the middle of inner race. This result is consistent with the simulation of defect on the outer race. The error between defect frequency (213 Hz) and theoretical frequency (217.1 Hz) is 1.8%, which indicates that the FFT of Y direction velocity of point B is effective.

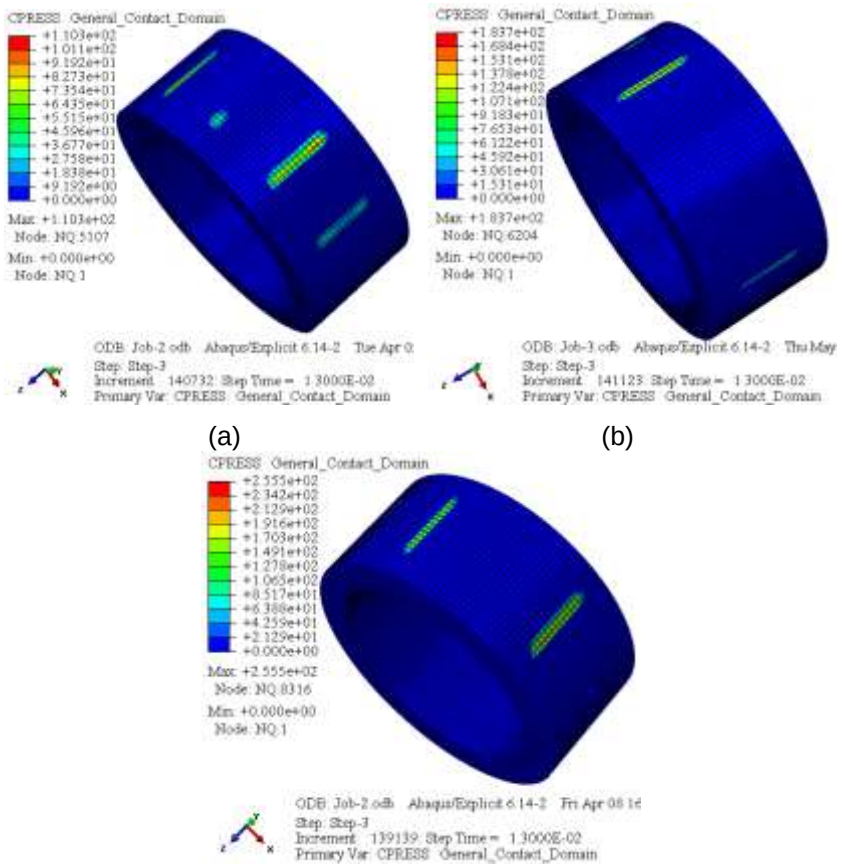

Figure 6. Contact Stress of Inner Race at 0.13s: (a) Normal Situation, (b) Edge Defect Situation (c) Middle Defect Situation

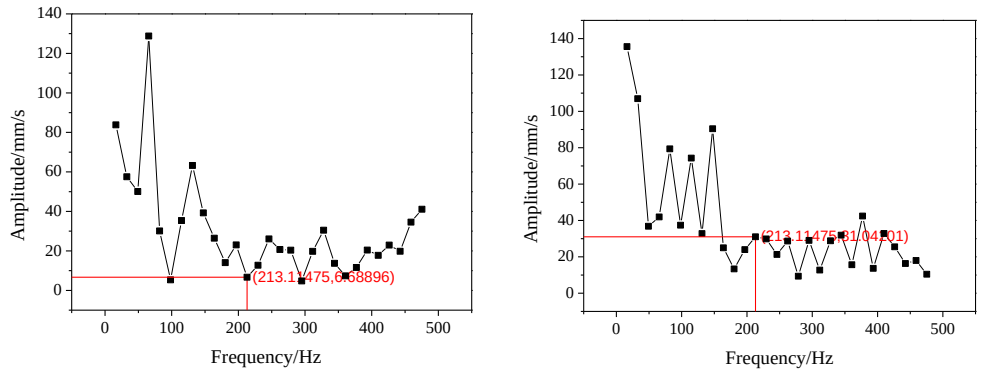

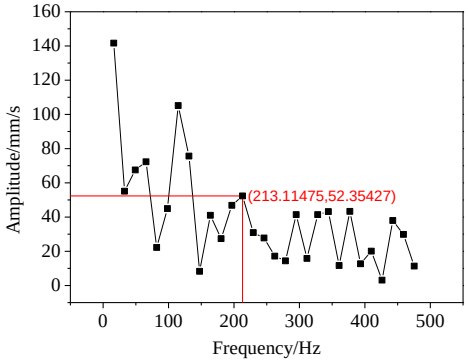

(c)

Figure 7. FFT of Y-direction Speed of Point B: (a) Normal Situation, (b) Edge Defect Situation, (c) Middle Defect Situation

5. Experimental Verification

5.1. Experimental Program

The vibration experiments of bearing NU308E are carried out on BVT-8 bearing vibration measuring instrument, as shown in Figure 8, and the experimental program is as follows:

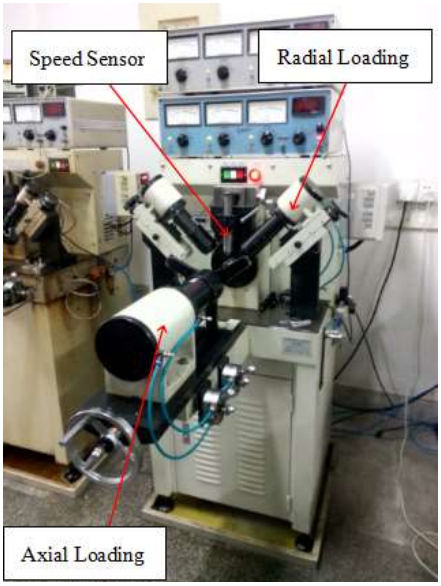

Figure 8. Bearing Vibration Measuring Instrument

(1) Prepare there bearing inner races, and number them. Then, grid out an edge defect with the diameter of 2 mm on the external surface of the No. 2 inner race, and a middle defect on the No. 3 inner race, as shown in Figure 9. Meanwhile, in order to reduce the experimental error, the same outer race, cage and rollers are used in the experiments, and just replace the inner race.

(2) Fix the bearing outer race, and use the radial loading system to apply radial load on the bearing outer race. The radial force applied to the outer race is 250 N and the revolving speed applied to inner race is1800 r/min. The test point of sensor is in the middle of the outer surface of outer race along the width direction. In order to extract the

peak velocity of different measuring point, the outer race need to be rotated a certain angle after each test.

(3) Finally, installing the bearing inversely and test again according to the above steps.

(a) (b) (c)

Figure 9. Defective Inner Race: (a) Normal, (b) Edge Defect, (c) Middle Defect

5.2. Experimental Result Analysis

Table 4 shows the test data of bearing speed, X_1, X_2 and X_3 represent the tested speed peak of the three times.

Table 4. Test Result of Velocity Peak of Bearing

No.	Installation	Vibration value(um/s)								
		Lower frequency 50～300HZ			Middle frequency 300～1800HZ			Higher frequency 1.8K～10KHZ		
		X_1	X_2	X_3	X_1	X_2	X_3	X_1	X_2	X_3
1	Positive	380	340	300	340	360	300	800	900	820
	Inversion	300	300	320	240	280	300	740	700	780
2	Positive	800	820	820	500	520	520	600	600	620
	Inversion	780	800	740	520	500	500	740	700	660
3	Positive	1300	1400	1400	620	580	640	720	740	660
	Inversion	1400	1500	1500	640	580	580	720	700	740

Average the data, and take the greater value of X between the positive and the inverted situation. The average value is shown in Table 5.

Table 5. Average Value of Velocity Peak

No.	Vibration value(um/s)		
	Lower frequency 50～300HZ	Middle frequency 300～1800HZ	Higher frequency 1.8K～10KHZ
1	340	333	840
2	813	500.6	700
3	1466	613	720

From Table 5, we know that, the peaks of velocity of the there situations change obviously at lower frequency stage of 50 ~ 300 Hz that has the consistency with the theoretical frequency 217.1 Hz and the simulation frequency 213 Hz.; the peaks of velocity increase when defect occurs, and the amplitude of middle defect increases larger than the one of edge defect. The increase of peak of velocity at middle frequency stage of 300 ~ 1800 Hz is less than the one at lower frequency stage, and the one at high frequency stage is the least.

The measured experimental peak of velocity is smaller than the simulation result of FFT analysis. The reason is that the experimental bearing is lubricated, that makes the bearing vibration and the measured peak reduce.

6. Conclusion

(1) The vibration also exists in the bearing without defect, and the existences of local defects make bearing stress fluctuation increase, which intensifies the bearing vibration. Due to the stress concentration at the position of defect, the defect is easy to extend, that will intensify the bearing vibration ulteriorly.

(2) To the situation of defective outer race, the stress fluctuation of outer race decreases when defect position moves from the middle of outer race to the edge. When defect occurs in the middle of outer race, the stress fluctuation is the largest. It means that the vibration and shock suffered by the bearing is the largest

(3) From the results of the displacement of time domain analysis of defective outer race and the velocity of frequency domain analysis of defective inner race, we know that the amplitudes increase at defect frequency, and the increased value when defect occurs in the middle of races is larger than the one when defect occurs on the edge of races. There are consistent regularity between experimental results and the simulation results, which verifies the validity of the model in this paper.

Acknowledgments

This paper is supported by National Natural Science Foundation of China (Grant No. 51504157); Natural Science Foundation of Shanxi province (2015021110); Youth Fund Project of Taiyuan University of Science and Technology (20143009) and Scientific and Technological Innovation Projects of Taiyuan University of Science and Technology (20145026).

References

[1] Z. Z. Wei. “Dynamic research and fault simulation on cylindrical roller bearing based on explicit dynamic”. Taiyuan University of Technology, Taiyuan, **(2013)**, pp. 8-30.
[2] M. Fadden P. D and S. J. D. “Model for the vibration produced by multiple point defects in a rolling element bearing”. Journal of Sound and Vibration, vol. 98, no. 2, **(1985)**, pp. 263-273.
[3] Z. L. le, T. L. Lin, and F. Li, “The dynamics simulation and failure analysis of rolling bearings”, Journal of Shanghai Jiao Tong University, vol. 41, no. 9, **(2007)**, pp. 1497- 1500.
[4] J. Sopanen and A. Mikola. “Dynamic model of a deep－groove ball bearing including localized and distributed defects-part 2: implementation and result”, Proceedings of the institution of mechanical engineers k-journal of multi-body dynamics. vol. 217, **(2003)**, pp. 213-223.
[5] Z. Z. Fang, Z. Y. Lu, L. Q. Guo and X. Bin, “Research on the dynamic simulation of local defects for rolling bearing outer ring”, Machine Design and Research, vol. 30, no. 2, **(2014)**, pp. 80-82.
[6] Z. G. Yuan, Z. Hong and C. Z. Yu, “Dynamic response of deep groove ball bearing with point defects”. Journal of Zhejiang University (Engineering Science), vol. 43, no. 8, **(2009)**, pp. 1497-1500.
[7] Y. Yang, D. Z. Shan, G. B. Liang and L. Heng, “Kinetics study on single point corrosion fault of rolling bearing for vibrating machine”. Bearing, no. 5, **(2015)**, pp. 41-46.
[8] D. Y. Bin, L. M. Fu and G. Qi, “Dynamics analysis on rolling element bearings with localized defects”, Heavy Machinery, no. 3, **(2012)**, pp. 148-152.
[9] Z. C. Jiu, Z. A. Hua, X. Y. Hua and X. Yong, “Dynamics analysis on defect bearings for railway freight based on LS－DYNA”, Bearing, no. 6, **(2015)**, pp. 7-11.

[10] G. Hui, "Study of fault diagnosis of rolling bearings based on the wavelet analysis", Tai Yuan University of Science and Technology, Taiyuan, **(2008)**, pp. 10-30.
[11] Z. H. Xin, Z. Hao and S. X. Jiang, "Research on Rolling Bearing Fault Diagnosis with Adaptive Frequency Selection based on LabVIEW", International Journal of Control and Automation, vol. 1, no. 3, **(2014)**, pp. 93-100.
[12] W. Xing, Q. X. Dong and L. B. Jin, "Rolling bearing fault diagnosis based on time-frequency feature parameters and wavelet neural network", International Journal of Control and Automation, vol. 8, no. 4, **(2015)**, pp. 45-52.
[13] X. Wei and Y. T. Qiang, "Analysis of contact mechanics characteristic of deep groove ball bearing", Journal of Mechanical Transmission, vol. 36, no. 10, **(2012)**, pp. 78-81.
[14] W. Jie, "Mechanical properties analysis of coated cylindrical roller bearing", Yan Shan University, Yanshan, **(2013)**.
[15] M. S. Patil, J. Mathew and P. K. R Ajendrakumar, "A theoretical model to predict the effect of the localized defect on vibrations associated with ball bearing", International Journal of Mechanical Sciences, vol. 52, **(2010)**, pp. 1193-1201.
[16] L. Yang, "Dynamic finite element simulation of bearing at service process", Lanzhou University of Technology, Lanzhou, **(2014)**.

